Molecular Crystals and Liquid Crystals

Publication details, including instructions for authors and subscription information:
http://www.tandfonline.com/loi/gmcl20

SIMPLE 4,4′-DIALKYL DERIVATIVES OF [bpy$MS_2C_6H_4$] (bpy = 2, 2′-BIPYRIDINE; M = Ni, Pt) EXHIBIT THERMOTROPIC MESOMORPHISM: THE RELATIONSHIP BETWEEN STRUCTURE AND PHASE BEHAVIOR

T. Matthew Cocker [a] & Robert E. Bachman [a]

[a] Department of Chemistry, Georgetown University, Box 571227, Washington, DC 20057-1227, USA

Version of record first published: 15 Jul 2010

To cite this article: T. Matthew Cocker & Robert E. Bachman (2004): SIMPLE 4,4′-DIALKYL DERIVATIVES OF [bpy$MS_2C_6H_4$] (bpy = 2, 2′-BIPYRIDINE; M = Ni, Pt) EXHIBIT THERMOTROPIC MESOMORPHISM: THE RELATIONSHIP BETWEEN STRUCTURE AND PHASE BEHAVIOR, Molecular Crystals and Liquid Crystals, 408:1, 1-19

To link to this article: http://dx.doi.org/10.1080/15421400490425711

Mol. Cryst. Liq. Cryst., Vol. 408, pp. 1–19, 2004

ISSN: 1542-1406 print/1563-5287 online
DOI: 10.1080/15421400490425711

Taylor & Francis
Taylor & Francis Group

SIMPLE 4,4′-DIALKYL DERIVATIVES OF [bpy$MS_2C_6H_4$] (bpy = 2, 2′-BIPYRIDINE; M = Ni, Pt) EXHIBIT THERMOTROPIC MESOMORPHISM: THE RELATIONSHIP BETWEEN STRUCTURE AND PHASE BEHAVIOR

*T. Matthew Cocker and Robert E. Bachman**†*
Department of Chemistry, Georgetown University, Box 571227, Washington, DC 20057–1227, USA

*Complexes of the general formula [{4,4′-$R_2C_{10}H_6N_2$}$MS_2C_6H_3R'$], where M = Ni or Pt, R is an alkyl chain, and R′ is either a H atom (bdt) or a CH_3 group (tdt), were prepared and shown to exhibit thermotropic poly- and mesomorphism. Complexes with short alkyl chains exhibit one or more crystal-to-crystal transitions. Complexes with R = $C_{17}H_{35}$ and R = H, CH_3 (i.e., **C_{17}Mbdt** and **C_{17}Mtdt**) possess soft crystalline phases, which were characterized by optical microscopy, differential scanning calorimetry, and variable temperature X-ray diffraction. The solid-state structures of several members of this series (**C_4Nibdt**, **C_6Nibdt**, **C_4Ptbdt**, **C_5Ptbdt**, **C_8Ptbdt**, **C_{13}Ptbdt**, and **C_{17}Pttdt**) were also characterized crystallographically. Irrespective of alkyl chain length, these complexes show essentially identical structures at both the molecular and supramolecular level. The inorganic cores form columnar stacks via π-π stacking, while the alkyl chains on the periphery of the columns adopt conformations that allow for efficient packing via interdigitation of chains from adjacent columns. Correlation of the phase behavior of these complexes with the solid-state structural information has led to the development of structure–property relationships linking specific structural features to the observed poly- and mesomorphism.*

Keywords: diimine complexes; metallomesogens; nickel; platinum

This work was supported by Georgetown University and the donors of the Petroleum Research Fund, administered by the ACS (#31945-G3). Funding for the purchase of the X-ray diffractometer was provided by the National Science Foundation (CHE-9115394) and Georgetown University. The authors wish to thank Timothy Swager, Hsiu-Fu Hsu, and Stephan Holger Eichhorn (MIT) for their assistance in obtaining the XRD data.

†Current Address: Department of Chemistry, The University of the South, 735 University Ave., Sewanee, TN 37383

*Corresponding Author. E-mail: rbachman@sewanee.edu

INTRODUCTION

Liquid crystals are widely recognized as a technologically important class of materials with applications in areas as diverse as flat panel displays, optical switches, sensors (thermometers), and solvents for both spectroscopy and chemical reactions [1]. While the vast majority of mesogenic* materials are based on organic molecules, there has been a growing interest in developing metal-containing liquid crystals (metallomesogens) over the last twenty years [3]. The central motivation behind this effort has been to combine the unique properties of transition-metal complexes (e.g., color, magnetism, redox behavior) with those associated with liquid crystallinity (e.g., responsiveness to environmental stimuli) [4]. Potential applications of these hybrid systems include magneto-optical devices, ferroelectrics, conducting materials, and nonlinear optical materials.

To date the majority of research on metallomesogens has focused on the use of "liquid-crystal-like" ligands. In these systems, the ligands employed usually possess a molecular architecture similar to that found in traditional organic mesogens, with two or more aromatic rings appended with multiple aliphatic groups [3]. In many cases the ligands themselves are mesogenic, while in other cases the metal is used to link two "protomesogenic" ligands to form a mesogenic system. While this approach has produced literally hundreds of interesting materials, the overall design philosophy remains ligand-centered; i.e., the principal design concern is that the ligand architecture be conducive to mesophase formation. There are noteworthy exceptions to this generalization; for example, simple transition-metal carboxylate complexes [5], tungsten oxide capped calixarene "cups" [6], and gold complexes with simple isonitrile ligands [7]. Such examples show that mesogenic behavior is more general than is widely believed and, perhaps more importantly, not restricted to systems that obey the structure-property relationships developed for organic systems. Given the increasing list of metallomesogens with novel metal-centered architectures, we decided to approach the problem of designing new types of metallomesogens from the "inverse" perspective of choosing a target chromophore and then asking how the structure of this chromophore must be modified to create a mesogenic variant. A central design criterion implicit in this approach is to keep the structural modifications as simple as possible in order to maximize the role of the chromophore in determining the properties of the resulting materials.

*The term "mesogenic" is frequently used interchangeably with the term "liquid-crystalline"; however, we are using the term in the broader sense of any phase with a degree of order intermediate between crystalline and isotropic (liquid). Examples include soft crystals, plastic crystals and rotator phases. For a complete discussion of the numerous phases available see Goodby et al. [2].

The specific chromophores we chose for this project were 2,2′-bipyridineplatinum(II)-1,2-benzenedithiolate and its nickel analog (**A**). We selected this system primarily for its many unique photophysical and electrochemical properties [8]. These include an intense color (arising from a strong charge transfer transition), photoluminescent behavior, a significant second-order hyperpolarizability, and novel redox and photo-redox behavior. A second reason for this choice of targets was the challenge of utilizing bipyridine ligands in the construction of metallomesogens. While bipyridine plays an almost ubiquitous role in coordination chemistry generally [9], it is rarely found as a component of metallomesogens [10]. Indeed, in several instances the coordination of a metal atom to a mesogenic free bipyridine ligand has resulted in the loss of the mesogenic properties [11].

As part of our effort to understand the minimum set of molecular features necessary for mesogenic behavior, we have placed an emphasis on

Diagram (A)

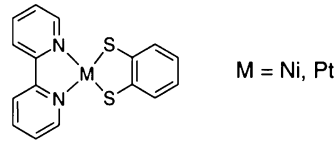

A

Scheme 1

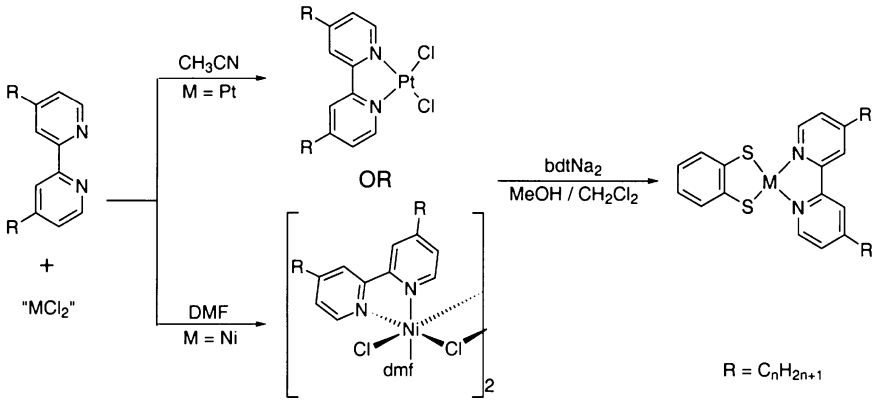

SCHEME 1 Synthetic route used to prepare the targeted $\mathbf{C_nMbdt}$ complexes.

developing structure-property relationships correlating both the molecular and supramolecular structure with phase behavior. In this report, we will discuss our initial attempts to create mesogenic systems through the attachment of simple *n*-alkyl chains at the 4 and 4′ positions of the bipyridine ligand of the chromophore. While these studies failed to produce any liquid crystalline variants, they did result in the production of several soft crystalline phases. Furthermore, the structural insight gained from crystallographic studies of several members of these new inorganic lipid materials has allowed us to develop the sought-after structure-property relationships to guide future efforts to produce liquid crystalline materials in a rational fashion.

RESULTS

Synthesis

The targeted molecules were assembled using a simple two-step protocol (Scheme 1). Coordination of the bipyridine ligands to either a nickel dichloride or a platinum dichloride fragment can be carried out efficiently by direct reaction of the two components in an appropriate solvent. For the nickel complexes, the addition of a strongly coordinating solvent such as DMF is necessary in order to produce a soluble product. TGA data obtained with fresh samples provide a DMF:metal ratio of 1:1, consistent with a formula of $[C_nNiCl_2(dmf)]_2$, which was confirmed by crystallography [12]. Samples stored for extended periods possess a lower DMF:metal ratio; however, this does not seem to affect their behavior in subsequent reactions. While DMF can be used for the synthesis of the platinum chloride complexes (**C_nPtCl_2**), we prefer more weakly coordinating solvents such as CH_3CN. While the rate of reaction is faster in the former, the isolation and purification is simpler in the latter.

For either series of chloride complexes, the dithiolate ligand can be coupled to the metal center by direct reaction of the sodium salt of the dithiolate with the bipyridine complex in a mixed $MeOH/CH_2Cl_2$ solvent system [13]. The final **C_nMbdt** complexes are easily purified by recrystallization from a mixture of cold $CHCl_3$ and hexanes, or by chromatography on silica. These complexes are moderately sensitive to photooxidation in solution; however, they can be handled quite well in low light levels, making rigorously anaerobic conditions unnecessary.

^{1}H NMR spectroscopy offers a simple and convenient diagnostic to follow the syntheses, as the signal associated with the 6,6′-protons shows a distinctive shift at each step of the process. This signal moves from 8.6 ppm in the free ligands to 9.22 ppm in **C_nPtCl_2** and then back to 8.9 ppm in **C_nPtbdt**. While the paramagnetic nature of the corresponding **C_nNiCl_2**

complexes prevents a meaningful comparison, the spectral behavior of the **C_nNibdt** complexes is essentially identical to their platinum analogs.

Molecular and Supramolecular Structure

Several of the dithiolate complexes, **C_nMbdt**, produced X-ray quality crystals by slow evaporation of either CH_2Cl_2 or $CHCl_3$ solutions. We undertook structural studies of those compounds that crystallized in order to examine how the presence of long alkyl chains influenced the supramolecular (crystal) structure.

Key crystallographic data for the compounds examined are reported in Table I.* At the molecular level, **C_nMbdt**(M = Ni, Pt) all form four-coordinate complexes with essentially square planar geometry (Figure 1) and bonding parameters in agreement with expectations [7,12]. The only exception to this generalization is **C_6Nibdt**, which displays a tetrahedral distortion of the square planar geometry at the metal center with a dihedral angle between the NiS_2 and NiN_2 planes of 16.1°. For comparison, the largest dihedral angles observed in the related nickel and platinum complexes that have been characterized is 5.9° (**bpyNibdt**) and 4.1° (**C_4Ptbdt**), respectively [12,13].

A significant molecular-level feature of these molecules is the relative disposition of the alkyl chains. In general, one of the chains extends from the inorganic core in an all-*anti* conformation with the carbon atoms of the aliphatic chain coplanar with the core. In a few examples (**C_5Ptbdt**, **C_{13}Ptbdt**, and **C_{17}Pttdt**), this alkyl chain is disordered over two essentially orthogonal orientations; however, even in these cases the chain propagation direction remains coplanar with the inorganic core. The position of the second alkyl chain is slightly more variable but may be generalized in the following manner: the chain is rotated around the C4(ring)-α-carbon bond in a pseudo-gauche fashion (C3-C4-C_α-C_β torsion = 59–91°), which initially orients the chain propagation direction roughly perpendicular to the plane of the inorganic core. In the complexes with alkyl chains longer than six carbons ($n \geq 6$), a second gauche conformation between the second and third methylene units (C_α-C_β-C_γ-C_δ torsion = 63.5–70.7°) realigns the chain propagation direction roughly parallel to both the inorganic core and the first alkyl chain. The energetically unfavorable gauche conformations necessary for the observed parallel orientation of the alkyl chains have been shown in other systems to be more than compensated for by the packing energy associated with this parallel orientation [14]. However, in the previously reported case the alkyl

*Full crystallographic details are available from the author and have been deposited with the Cambridge Crystallographic Database, quote reference Nos. 211032–211038

TABLE I Crystallographic Data for **C_nNibdt (n = 4, 6) C_nPtbdt (n = 4, 5, 8,**

	C_4Nibdt	C_6Nibdt	C_4Ptbdt
Empirical formula	$C_{24}H_{28}N_2NiS_2$	$C_{28}H_{36}N_2NiS_2$	$C_{24}H_{28}N_2PtS_2$
Formula weight	467.31	523.42	603.69
Temperature (K)	173	173	173
Crystal system	Triclinic	Triclinic	Monoclinic
Space group	P-1	P-1	P2(1)/c
Unit cell dimensions (Å, deg)	a = 9.244(5) α = 78.46(6) b = 9.729(6) β = 79.98(7) c = 13.235(10) γ = 73.52(6)	a = 8.532(3) α = 99.63(3) b = 11.436(5) β = 105.20(3) c = 15.269(7) γ = 108.50(2)	A = 9.232(3) B = 23.915(5) β = 101.887(11) C = 10.234(2)
Volume ($Å^3$)	1109.4(13)	1311.4(9)	2211.1(9)
Z	2	2	4
Absorption coefficient (mm^{-1})	1.076	0.918	6.548
Reflections collected	12339	14467	25764
Independent reflections (Rint)	3188 (0.0544)	6132 (0.0225)	5455 (0.0664)
Final R indices (obsd. data)	R1 = 0.0603, wR2 = 0.1477	R1 = 0.0405, wR2 = 0.0833	R1 = 0.0322, wR2 = 0.0623
Goodness of fit (GOF)	0.980	1.126	0.966

13) and **C_{17}Pttdt**

C_5Ptbdt	C_8Ptbdt	C_{13}Ptbdt	C_{17}Pttdt
$C_{26}H_{32}N_2PtS_2$	$C_{32}H_{44}N_2PtS_2$	$C_{42}H_{64}N_2PtS_2$	$C_{51}H_{82}N_2PtS_2$
631.75	715.90	856.16	982.40
173	173	173	173
Triclinic	Triclinic	Triclinic	Triclinic
P-1	P-1	P-1	P-1
a = 9.475(5) α = 73.43(3) b = 10.181(6) β = 74.30(2) c = 14.128(6) γ = 71.70(3) 1215.4(11) 2 5.960	a = 8.924(4) α = 75.67(5) b = 9.834(4) β = 79.77(3) c = 18.420(11) γ = 76.62(4) 1511.3(12) 2 4.804	a = 8.8137(9) α = 95.037(2) b = 9.9514(10) β = 95.783(2) c = 23.437(2) γ = 100.761(2) 1997.2(3) 2 3.648	a = 8.782(5) α = 89.95(7) b = 10.043(5) β = 84.24(7) c = 27.948(18) γ = 80.16(5) 2416(2) 2 3.025
13770	17295	22867	28202
5800 (0.0440)	7212 (0.0693)	8118 (0.0511)	8232 (0.1025)
R1 = 0.0398, wR2 = 0.0744 0.944	R1 = 0.0567, wR2 = 0.1256 0.932	R1 = 0.0429, wR2 = 0.0892 0.913	R1 = 0.0859, wR2 = 0.2055 1.039

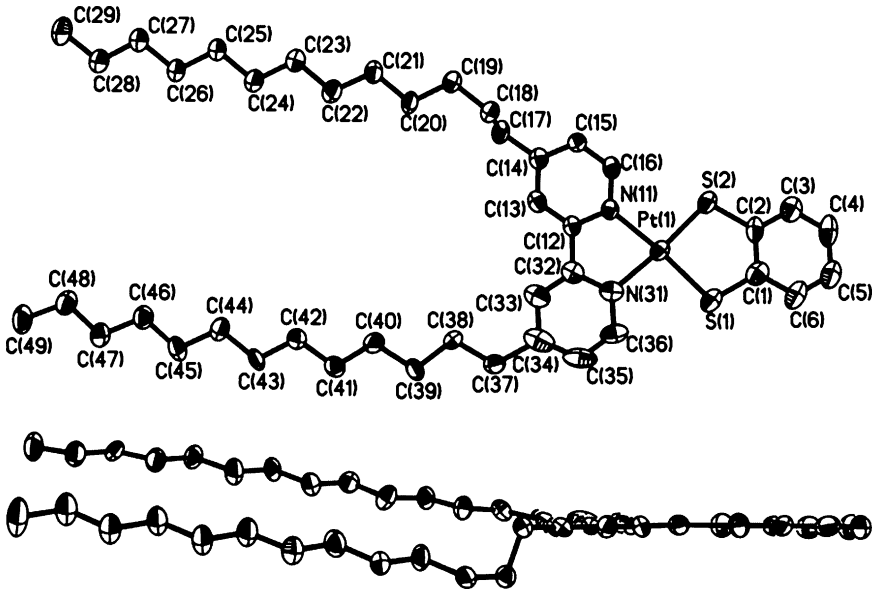

FIGURE 1 Thermal ellipsoid plots (50% probability) of **C_{13}Ptbdt** showing both the molecular geometry and the atom-labeling scheme.

chains aggregated intramolecularly, while in this work the parallel alkyl chains create a well-defined hydrophobic cleft and the stabilizing interactions between alkyl chains are intermolecular in nature (vida infra).

Since key structural features of these complexes are conserved between examples with widely different alkyl chain lengths, we propose that their molecular structure can be generalized as an acentric disk with two offset but parallel tails (see Figure 1). The overall supramolecular architecture can then be thought of as being derived from the microsegregation of the inorganic core (the disk) and the aliphatic tails of the molecules, as well as the intermolecular association of like parts of the molecules. This concept is particularly easy to see in the systems with the longest alkyl chains, **C_{13}Ptbdt** and **C_{17}Ptbdt**. The aggregation of the inorganic cores results in the formation of tilted columns with an H-like shape (Figure 2). The forces responsible for the this stacking are most likely π-π type interactions involving the bipyridine fragments and the platinum-sulfur ring systems, which have been shown to have some aromatic character [8,15]. The interplanar separation between the cores averages 3.42 Å (ranging from 3.40 to 3.46 Å) with the ring systems coplanar. The columnar stacks are then packed together such that alkyl chains achieve a close-packing arrangement via interdigitation of chains from adjacent columns.

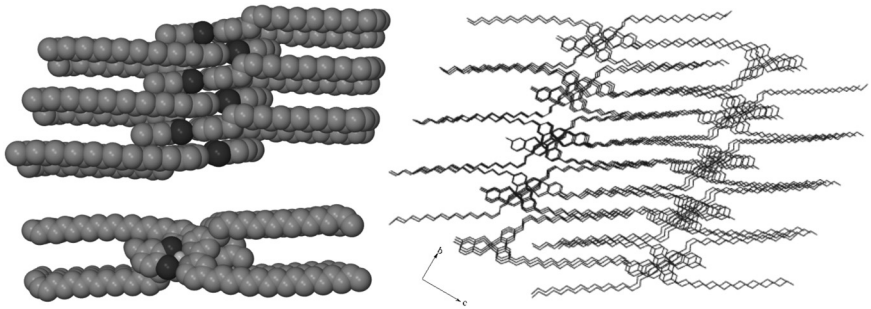

(a) (b)

FIGURE 2 (a) Two orthogonal space-filling views of a single column of $\mathbf{C_{17}Pttdt}$. The sulfur atoms are tagged black to highlight the location of the dithiolate moiety. Note the H-shape of the column in the top view. (b) A view down the crystallographic a-axis illustrating the packing of the columns of $\mathbf{C_{17}Pttdt}$, which also illustrates the interdigitated packing of the alkyl chains.

The packing of the alkyl chains is reminiscent of that seen in pure n-alkanes and other related systems [16]. In particular, Serrano and coworkers have reported a similar packing motif for a series of mesogenic salicylaldimine complexes [17].

Thermal Phase Behavior

Differential scanning calorimetry (DSC) indicates that essentially all of the $\mathbf{C_nMbdt}$ complexes with $n \geq 6$ exhibit temperature-dependent polymorphism. For $6 \leq n \leq 12$, these phase changes take the form of crystal-to-crystal (Cr-Cr) transitions that are only observed on the first heating cycle of samples freshly crystallized from solution (see experimental section for details). For $n \geq 13$ (i.e., $\mathbf{C_{13}Mbdt}$, $\mathbf{C_{17}Mbdt}$ (M = Ni or Pt), and $\mathbf{C_{17}Pttdt}$), significantly smaller enthalpies are observed for the transition to the isotropic phase (Table II), suggesting that the intermediate phases in these materials are mesogenic rather than crystalline. In order to

TABLE II Thermal Phase Behavior for $\mathbf{C_nNibdt}$, $\mathbf{C_nPtbdt}$, and $\mathbf{C_nPttdt}$ (n = 13, 17)

C_{17}Nibdt	$Cr_1 \overset{83^\circ C}{\longrightarrow} Cr_2 \overset{102^\circ C(41.0KJ/mol)}{\longrightarrow} CoI_h \overset{119^\circ C(6.8KJ/mol)}{\longrightarrow} I$
C_{13}Ptbdt	$Cr_1 \overset{104^\circ C(23.9KJ/mol)}{\longrightarrow} Cr_2 \overset{172^\circ C(16.7KJ/mol)}{\longrightarrow} I$
C_{17}Ptbdt	$Cr_1 \overset{82^\circ C}{\longrightarrow} Cr_2 \overset{104^\circ C(60.6KJ/mol)}{\longrightarrow} CoI_h \overset{155^\circ C(3.9KJ/mol)}{\longrightarrow} I$
C_{17}Pttdt	$Cr_1 \overset{73^\circ C}{\longrightarrow} Cr_2 \overset{88^\circ C(27.9KJ/mol)}{\longrightarrow} CoI_h \overset{170^\circ C(6.5KJ/mol)}{\longrightarrow} I$

qualitatively assess this possibility, we examined the phase behavior of these materials with polarizing optical microscopy (POM). Consistent with their slightly larger enthalpies of transition, the intermediate phases of **C_{13}Mbdt** (M = Ni, Pt) appear to be crystalline in nature. In contrast, the intermediate phases of **C_{17}Mbdt** (M = Ni, Pt) and **C_{17}Pttdt** will flow and deform slowly under an applied shear stress, supporting the assignment of these phases as mesogenic. The fine-grained texture (Figure 3) observed for these systems in the POM combined with their high viscosity is suggestive of a highly ordered phase [18].

In order to better understand the nature of these thermotropic transitions, we examined the phase behavior of representative complexes by variable-temperature X-ray diffraction (VT-XRD). For **C_6Nibdt**, the diffraction results confirm the crystalline nature of the high-temperature morph observed on the first heating cycle. Additionally, this high-temperature morph and the morph formed from the melt are identical (Figure 4). Interestingly, while there is a significant difference in the XRD patterns of the two morphs, two peaks, at circa 14.0 and 3.5 Å, remain constant across this monotropic phase transition. The larger of these values corresponds well to the length of the long axis (see Figure 2) of the H-shaped column observed in the solid state, while the shorter agrees well with the core–core separation within the columns. Hence, it seems likely that the columnar motif is preserved in the second morph and that the observed phase transition involves a rearrangement of the column packing and/or the alkyl chains.

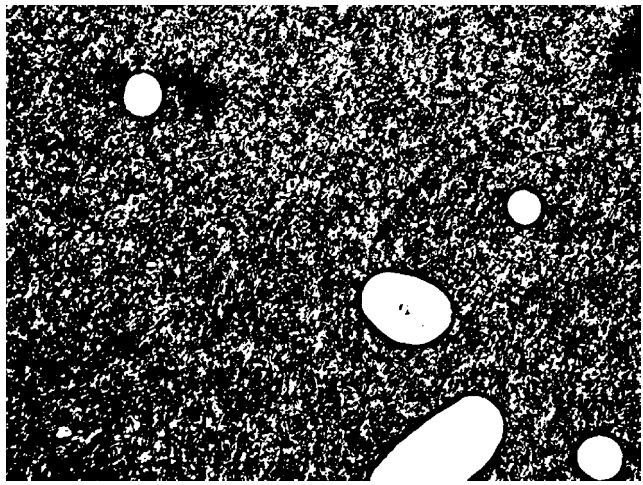

FIGURE 3 Polarized optical micrograph of **C_{17}Ptbdt** at 120°C on the cooling cycle showing the fine-grained texture typical of several highly ordered phases.

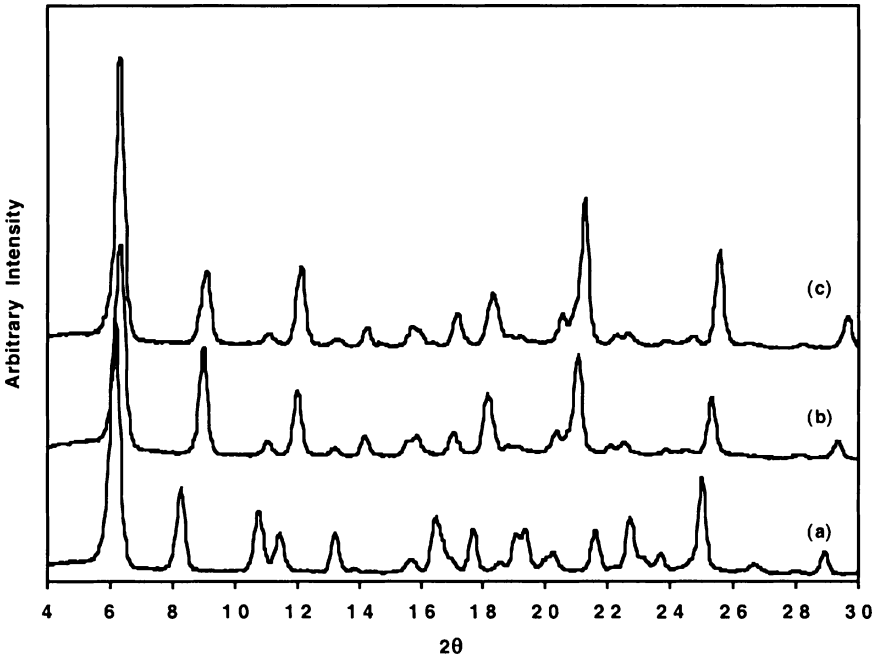

FIGURE 4 Variable temperature powder XRD traces for **C_6Nibdt**: (a) at 120°C on the initial heating cycle, (b) at 155°C on the initial heating cycle, and (c) at 120°C on the initial cooling cycle. The traces are offset along the intensity axis for clarity.

Consistent with its designation as a mesophase, the XRD pattern (Figure 5) of the high temperature phase of **C_{17}Ptbdt** shows a significant decrease in the number of peaks present and a concomitant increase in the peak widths relative to the room temperature phase. However, the distinct peaks in the high angle region, notably those at d = 4.73 and 4.12 Å, rule out the assignment of this phase as liquid crystalline; rather, it is best characterized as soft crystalline. The ratios of the low-angle peak positions (1: $\sqrt{3}$: $\sqrt{7}$: $\sqrt{16}$) suggest a columnar hexagonal packing motif. The two high-angle peaks mentioned above are characteristic of correlated alkyl chain packing [18]. A third high-angle peak at 3.58 Å is consistent with the separation typically seen for both π-π stacking [19] and Pt-Pt interactions in square planar complexes [20]. It is also interesting to note that this latter peak decreases from approximately 3.75 Å to 3.58 Å going from the solid (Figure 5(a)) to the mesophase (Figure 5(b)), while the two former peaks, associated with the alkyl chain contacts, increase slightly. These changes are consistent with a solid-to-liquid-like transition of the alkyl portion of the molecule coupled with a strengthening of the core–core interactions.

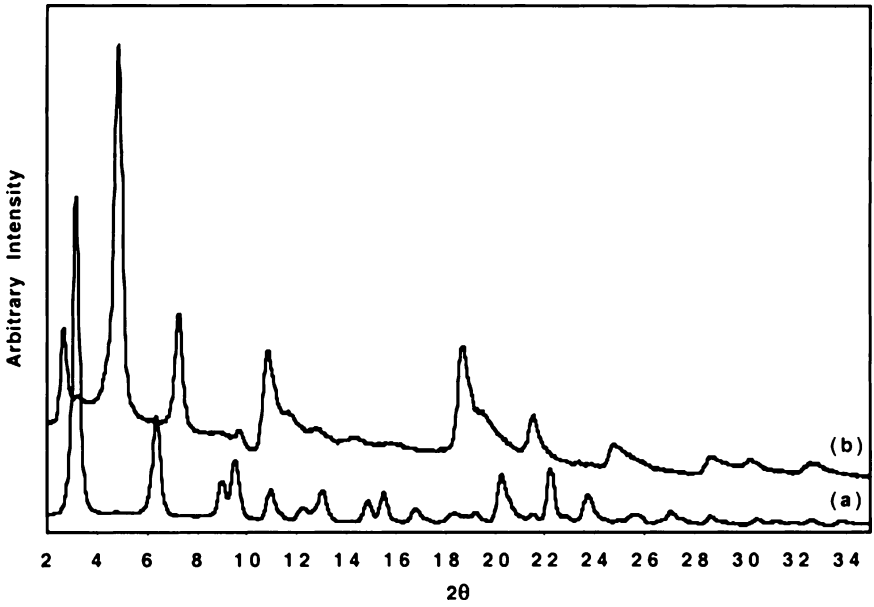

FIGURE 5 Variable temperature powder XRD traces for **C_{17}Ptbdt**, (a) at 35°C and (b) at 120°C. The traces are offset along the intensity axis for clarity.

Assuming a hexagonal packing motif and assigning the lowest angle peak ($2\theta = 2.69°$, d = 32.8 Å) as (001) yields a lattice constant of 37.9 Å, which agrees reasonably well with the value estimated for the long axis of the H-shaped column (36.4 Å) from the solid-state structure of **C_{17}Pttdt**.

DISCUSSION

Comparing the thermal behavior of the longest chain length members of the series, **C_{17}Nibdt** and **C_{17}Ptbdt**, it is clear that the melting (solid to mesophase) transition (Table II) is essentially unaffected by the identity of the metal atom. In contrast, the clearing (mesophase to isotropic) transition occurs at a substantially lower temperature in the nickel system (119°C versus 155°C). Given the invariance of the melting transition, we believe that it involves primarily a "melting" of the alkyl chains and a reorganization of the columnar structure from rectangular to hexagonal. The dependence of the clearing transition on the identity of the metal atom suggests that this process involves the disruption of the core–core interactions and consequently disruption of the columnar structure. There are two possibilities for how the change in metal atom could influence this process. A tetrahedral distortion of the molecular core, such as that seen in

the solid-state structure of **C_6Nibdt**, would presumably weaken the π-π stacking interactions between the bipyridine rings and destabilize the columnar packing necessary for mesophase formation in these systems. Alternatively, if the decrease in the core–core stacking distance seen in the XRD measurements of **C_{17}Ptbdt** were accompanied by a lateral shift of the cores, there is the possibility for the formation of metal-metal interactions. Such interactions have been shown to be favorable in square-planar d^8 metal complexes and are more significant for platinum than for the lighter members of the group [20]. Regardless of the exact mechanism responsible for the differences in the thermal behavior, these results indicate that the clearing temperature can be tuned by simply changing the identity of the metal atom.

As has been mentioned previously, the H-shape of the columns leaves a significant free volume, which is satisfied by interdigitation of the alkyl chains of neighboring columns, which is most likely at least partially maintained in the mesophase. We believe that this relatively extensive intermolecular entanglement is a primary reason that these materials form highly viscous soft crystalline, rather than liquid crystalline, phases. Hence, it should be possible to both lower transition temperatures and the viscosity of the mesophase by modifying the aliphatic groups to prevent, or at least decrease, the degree of interdigitation.

C_{17}Pttdt was prepared specifically to test the validity of this prediction. The addition of a single methyl group to the dithiolate ligand produced a significant drop in T_m (from 104°C for **C_{17}Ptbdt** to 83°C for **C_{17}Pttdt**) with little impact on the clearing temperature. Furthermore, the solid-state structure of **C_{17}Pttdt** shows that this additional methyl group forms an unfavorably close contact (approximately 3.0 Å) with the alkyl chain from a neighboring column. The repulsive nature of this close contact correlates well with the observed change in phase behavior.

CONCLUSIONS

We have prepared a new series of inorganic lipids by appending long aliphatic chains to diimine-dithiolate complexes of platinum and nickel. Many of these complexes display a rich thermotropic polymorphism, and a few display thermotropic mesophases in the form of hexagonal columnar soft-crystalline phases. Detailed structural studies on several members of this series have allowed us to develop a reasonably robust structure–property relationship correlating molecular and supramolecular structure with phase behavior. Additional studies are currently underway to use the insights gained through this work to prepare liquid crystalline variants of these complexes in a rational fashion.

APPENDIX: SUPPORTING INFORMATION AVAILABLE

This appendix contains synthetic details for preparation of the alkylated bipyridine ligands as well as complete spectral data for all metal complexes (**[C_nNiCl$_2$(dmf)]$_2$** , **C_nPtCl$_2$**, **C_nMbdt**, **C_nMtdt**). Also included are details of crystallographic refinement and tables of crystal data, positional parameters, bond distances and angles, and anisotropic displacement parameters for **C_4Nibdt**, **C_6Nibdt**, **C_4Ptbdt**, **C_5Ptbdt**, **C_8Ptbdt**, **C_{13}Ptbdt**, and **C_{17}Pttdt**. An X-ray crystallographic file (CIF).

Experimental

General Considerations

All manipulations were carried out under an atmosphere of anhydrous deoxygenated nitrogen unless stated otherwise. Solvents were distilled from the appropriate drying agents under nitrogen prior to use [21]. The following reagents were available commercially and used as received from the supplier: K_2PtCl_4 (Alfa, Ward Hill, MA, USA); 2.5 M n-butyllithium in hexane, diisopropylamine, 4-picoline (Acros, Morris Plains, NJ, USA); 3,4-toluenedithiol, *n*-$C_nH_{2n+1}Br$ (n = 2–8, 12) (Aldrich, St. Louis, MO, USA); *n*-$C_{16}H_{33}Br$ (Humphrey, East Rutherford, NJ, USA). Lithium diisopropylamide (LDA) was made by adding n-butyllithium to a 1% excess of diisopropylamine in ether and warming the mixture to reflux for 24 h. The product was then recovered as a white solid by filtration and dried in vacuo for 24 h at 60°C. Anhydrous $NiCl_2$ was prepared either by literature methods [22] or by simply heating $NiCl_2{\cdot}6H_2O$ to >230°C for 7 days. In both cases the resulting tan solid showed no weight loss up to 200°C by TGA. 4,4′-dimethyl-2,2′-bipyridine was synthesized via a modified version of the method of Sasse [23]. The ligands with extended alkyl chains were in turn prepared from 4,4′-dimethyl-2,2′-bipyridine using a modification of the procedure developed by Garelli and Vierling [24] (please refer to the supplementary materials for details). 1,2-benzenedithiol was prepared according to literature procedures [25] and converted to the corresponding sodium dithiolate salt by reaction with NaH in ether. Purity was assessed by observing the thermal behavior of the complexes; a compound was considered pure when constant and reproducible transition temperatures were observed [26].

Instrumentation

^{1}H and ^{13}C NMR spectra were obtained on a Varian Mercury 300 spectrometer in $CDCl_3$ unless otherwise noted. Chemical shifts are reported in ppm (δ) referenced relative to TMS (δ = 0 ppm). Differential scanning calorimetry (DSC) measurements were made under a nitrogen atmosphere

using open aluminum pans on a TA Instruments 2910 DSC. Thermal gravimetric analyses (TGA) were obtained using platinum pans on a TA Instruments 2050 TGA. Polarizing optical microscopy was performed using a Leitz 585 SM-LUX-POL microscope equipped with crossed polarizers, a Leitz 350 heating stage, an Omega HH21 microprocessor thermometer connected to a J-K-T thermocouple, and an RS Photometrics CoolSNAP CCD camera.

Synthesis of $[C_nNiCl_2(dmf)]_2$(C_n = 4,4′-$(C_nH_{2n+1})_2$-2, 2′-$C_{10}H_6N_2$), Typical Procedure

$[LNiCl_2(dmf)]_2$ was prepared via a modified version of the method described previously [27]. Equimolar amounts of the free ligand and anhydrous $NiCl_2$ were dissolved/suspended in THF and heated to reflux for 18–24 h. The resulting pale green suspension was cooled to RT, and the solvent was removed in vacuo. The solids were taken up in DMF and filtered. For chain lengths less than 8 carbons, addition of cold ether resulted in precipitation of the product as a dark green solid. For those systems with alkyl chains of eight or more carbons, an additional recrystallization from cold (−20°C) $CHCl_3$/hexane was required. Yields were typically in the range of 70–85%, although some final yields were lower due to recrystallization losses. No attempt was made to optimize the yields. Detailed characterization data for each compound is available as supplementary material.

Synthesis of C_nPtCl_2, (C_n = 4,4′-$(C_nH_{2n+1})_2$-2,2′-$C_{10}H_6N_2$)

Method A. Equimolar amounts of the free ligand and K_2PtCl_4 were heated to reflux in approximately 80 ml CH_3CN for 5 days. The color of the solution slowly turned from pale red to bright yellow during this time. After allowing the reaction mixture to cool, 200 ml of cold water was added, leading to precipitation of the product as a yellow solid. The solid was collected by filtration and dried by washing with methanol. The crude product was further purified by chromatography on silica using a ramped mixture of hexane/$CHCl_3$ as the elutant.

Method B. Equimolar amounts of the free ligand and K_2PtCl_4 were heated to 110°C in 50 ml DMF for 18 h. The color of the solution turned from pale red to bright yellow during the reaction. After allowing it to cool to RT, the reaction mixture was concentrated in vacuo to give a yellow paste. 100 ml of H_2O was added and the mixture was then extracted with 3×100 ml of CH_2Cl_2. The combined organic fractions were dried over $MgSO_4$ and evaporated to yield a yellow solid. The crude product was further purified by chromatography on silica using a ramped mixture of hexane/$CHCl_3$ as the elutant.

The final isolated yields ranged widely, from approximately 40 to 95%. This variation is primarily the result of recrystallization losses during purification. No attempt was made to optimize the yields. Detailed characterization data for each compound is available as supplementary material. Representative NMR data (**$C_{17}PtCl_2$**)—^{1}H NMR: 0.88 (t, 6H, $J = 6.3$ Hz), 1.26 (m, 56H), 1.74 (m, 4H), 2.80 (t, 4H, $J = 7.5$ Hz), 7.23 (d, 2H, $J = 6.0$ Hz), 7.85 (s, 2H), 9.29 (d, 2H, $J = 6$ Hz); ^{13}C NMR: 14.24, 22.78, 29.32, 29.43, 29.61, 29.76 (9 C), 29.90, 31.99, 35.89, 123.47, 126.47, 148.43, 156.29, 156.32.

Synthesis of $C_nMS_2C_6H_4$(C_n = 4,4′-(C_nH_{2n+1})$_2$-2,2′-$C_{10}H_6N_2$, M = Ni, Pt), Typical Procedure [13]

A solution of $bdtNa_2$ dissolved in MeOH was added with stirring to either $[C_nNiCl_2(dmf)]_2$ or C_nPtCl_2 dissolved in CH_2Cl_2. The resulting mixture immediately changed to a dark purple color. The reaction was heated to reflux for 3 h and then allowed to cool overnight. After removing the solvents in vacuo, the dark purple residue was redissolved in CH_2Cl_2 and filtered. Evaporation of the filtrate in vacuo and recrystallization from cold $CHCl_3$/hexane yields the product as a deep reddish purple solid. Isolated, but unoptimized, yields typically ranged from 55 to 98%. Detailed characterization data for each compound is available as supplementary material. Representative spectral data (**$C_{17}Ptbdt$**)—UV-Vis: λ_{max} ($CHCl_3$) 570 nm; ^{1}H NMR: 0.88 (t, 6 H, $J = 6.3$ Hz), 1.26 (m, 56 H), 1.71 (m, 4 H), 2.70 (t, 4 H, $J = 7.8$ Hz), 6.81 (dd, 2 H, $J = 6.0$, 3.0 Hz), 7.21 (d, 2 H, $J = 5.1$ Hz), 7.41 (dd, 2 H, $J = 6.0$, 3.0 Hz), 7.76 (s, 2 H), 9.03 (d, 2 H, $J = 6$ Hz); ^{13}C NMR: 14.25, 22.79, 29.36, 29.45, 29.65, 29.74(9 C), 29.86, 32.00, 35.78, 121.71, 123.09, 126.98, 127.98, 142.12, 147.74, 154.61, 155.08.

X-ray Crystallography

All X-ray data were collected on a Bruker-AXS SMART CCD system equipped with a Bruker-AXS LT2 low temperature device. The crystals were grown by the slow evaporation of halogenated solvents (CH_2Cl_2 or $CHCl_3$) and mounted on glass fibers using epoxy cement. The initial unit cell determination and data collection were performed as described previously [28]. Absorption corrections were made on the basis of equivalent reflection measurements using Blessing's method as incorporated into the program SADABS [29]. The structures were solved and refined on F^2 using the SHELXTL package (Ver. 5.05) and visualized using the X-SEED graphics package [30]. Unless otherwise noted, all nonhydrogen atoms were well behaved and refined anisotropically. The hydrogen atoms were included in calculated positions using a standard riding model. The essential crystallographic data for the compounds studied are provided in Table 1. Complete information is available as supplementary materials.

X-ray Powder Diffraction

Variable temperature X-ray powder diffraction (XRD) patterns for **C_6Nibdt** and **C_{17}Ptbdt** were collected on an Inel CPS-120 diffractometer using Cu K_α radiation ($\lambda = 1.54178$ Å), calibrated with mica, and equipped with a home-built sample thermostat unit. Finely powdered samples were packed into 1 mm capillaries (Charles Supper Company, Natick, MA, USA). The diffraction patterns were collected in each of the appropriate temperature ranges on both the heating and cooling cycles.

REFERENCES

[1] (a) *The Economist*, May 22, 1999, p. 68.
(b) Sage, I. C., Crossland, W. A., Wilkinson, T. D., Gleeson, H. F., Leigh, W. J., & Workentin, M. S. (1998). *Handbook of Liquid Crystals*, Vol. 1, Demus, D., Goodby, J., Gray, G. W., Speiss, H.-W., & Vill, V. (Eds.), (Weinheim: Wiley-VCH) Chap. 9, pp. 731–896 and references therein.

[2] Goodby, J. W. & Gray, G. W. (1998). *Handbook of Liquid Crystals*, Vol. 1 Demus, D., Goodby, J., Gray, G. W., Speiss, H.-W., & Vill, V. (Eds.), (Weinheim: Wiley-VCH) Chap. 2, pp. 17–23.

[3] (a) Giroud-Godquin, A. & Maitlis, P. M. (1991). *Angew. Chem., Int. Ed. Engl.*, *30*, 375–402.
(b) Espinet, P., Esteruelas, M. A., Oro, L. A., Serrano, J. L., & Sola, E. (1992). *Coord. Chem. Rev.*, *117*, 215–275.
(c) Hudson, S. A. & Maitlis, P. M. (1993). *Chem. Rev. 93*, 861–885.
(d) Serrano, J. L. (1996). *Metallomesogens* (Weinheim: VCH)
(e) Hoshino, N. (1998). *Coord. Chem. Rev.*, *174*, 77–108.
(f) Collinson, S. R. & Bruce, D. W. (1999). *Pers Supramol. Chem.*, *5*, 285–369.
(g) Demus, D. (2001). *Mol. Cryst. Liq. Cryst. Sci. Tech., Sec. A, 364*, 25–91.
(h) Binnemans, K. & Goerller-Walrand, C. (2002). *Chem. Rev.*, *102*, 2303–2345.

[4] Bruce, D. W. (1993). *J. Chem. Soc., Dalton Trans.*, 2983–2989.

[5] (a) Chisholm, M. H. (2000). *Acc. Chem. Res. 33*, 53–61.
(b) Baxter, D. V., Clayton, R. H., Chisholm, M. H., Huffman, J. C., Putilina, E. F., Tagg, S. L., Wesemann, J. L., & Zwanziger, J. W. (1994). *J. Am. Chem. Soc.*, *116*, 4551–4566.
(c) Barbera, J., Esteruelas, M. A., Levelut, A. M., Oro, L. A., Serrano, J. L., & Sola, E. (1992). *Inorg. Chem.*, *31*, 732–737.
(d) Giroud-Godquin, A. M., Marchon, J. C., Guillon, D., & Skoulios, A. (1984). *J. Phys. Lett.*, *45*, L681-L684.

[6] Xu, B. & Swager, T. M. (1993). *J. Am. Chem. Soc.*, *115*, 1159–1160.

[7] (a) Bachman, R. E., Fioritto, M. S., Fetics, S. K., & Cocker, T. M. (2001). *J. Am. Chem. Soc.*, *123*, 5376–5377.
(b) Coco, S., Espinet, P., Falagán, S., & Martín-Alvarez, J. M. (1995). *New J. Chem.*, *19*, 959–964.
(c) Coco, S., Espinet, P., Falagán, S., & Martín-Alvarez, J. M., & Levelut, A.-M. (1997). *J. Mater. Chem.*, *7*, 19–23.

[8] (a) Base, K., Tierney, M. T., Fort, A., Muller, J., & Grinstaff, M. W. (1999). *Inorg. Chem.*, *38*, 287–289.
(b) Paw, W., Cummings, S. D., Mansour, M. A., Connick, W. B., Geiger, D. K., & Eisenberg, R. (1998). *Coord. Chem. Rev.*, *171*, 125–150.

(c) Cummings, S. D., Cheng, L.-T., & Eisenberg, R. (1997). *Chem. Mater.*, *9*, 440–450.
(d) Connick, W. B. & Gray, H. B. (1997). *J. Am. Chem. Soc.*, *119*, 11620–11627.
(e) Cummings, S. D. & Eisenberg, R. (1996). *J. Am. Chem. Soc.*, *118*, 1949–1960.
(f) Zuleta, J. A., Burbery, M. S., & Eisenberg, R. (1990). *Coord. Chem. Rev.*, *97*, 47–64.

[9] (a) Kaes, C., Katz, A. & Hosseini, M. W. (2000). *Chem Rev.*, *100*, 3553–3590.
(b) Reedijk, J. (1987). *Comprehensive Coordination Chemistry Vol. 2*, Wilkinson, G., Gillard, R. D. & McCleverty, J. A. (Eds.), (Oxford: Pergammon) pp. 73–98.
(c) McWhinnie, W. R. & Miller, J. D. (1969). *Advan. Inorg. Chem. Radiochem.*, *12*, 135–215.

[10] (a) Ziessel, R. (2001). *Coord. Chem. Rev. 216*, 195–223.
(b) El-ghayoury, A., Douce, L., Skoulios A., & Ziessel, R. (1998). *Angew. Chem. Int. Ed.*, *37*, 1255–1258.
(c) El-ghayoury, A., Douce, L., Skoulios A., & Ziessel, R. (1998). *Angew. Chem. Int. Ed.*, *37*, 2205–2208.
(d) Neve, F., Ghedini, M., Francesangeli O., & Campagna, S. (1998). *Liq. Cryst.*, *24*, 673–680.
(e) Rowe, K. E. & Bruce, D. W. (1996). *J. Chem. Soc., Dalton Trans.*, 3913–3915.
(f) Bruce, D. W. & Rowe, K. E. (1995). *Liq. Cryst.*, *18*, 161–163.
(g) Kuboki, T., Araki, T., Yamada M., & Shiraishi, S. *Bull. Chem. Soc. Jpn.*, *67*, 948–955.

[11] (a) Rowe, K. E. & Bruce, D. W. *Mol. Cryst., Liq. Cryst.*, *326*, 15–40.
(b) Rowe, K. E. & Bruce, D. W. (1996). *Liq. Cryst.*, *20*, 183–193.
(c) Douce, L., Ziessel, R., Seghrouchni, R., Skoulios, A., Campillos, E., & Deschenaux, R. (1996). *Liq. Cryst.*, *20*, 235–242.

[12] Cocker, T. M. (2000). Ph.D. Thesis, Georgetown University, Washington, DC.

[13] Cocker, T. M. & Bachman, R. E. (2001). *Inorg. Chem.*, *40*, 1550–1556.

[14] Abdallah, D. J., Bachman, R. E., Perlstein, J., & Weiss, R. G. (1999). *J. Phys. Chem. B*, *103*, 9269–9278.

[15] (a) Zuleta, J. A., Bevilacqua, J. M., Proserpio, D. M., Harvey, P. D., & Eisenberg, R. (1992). *Inorg. Chem.*, *21*, 2396–2404.
(b) Sawyer, D. T., Srivatsa, G. S., Bodini, M. E., Schaefer, W. P., & Wing, R. M. (1986). *J. Am Chem. Soc.*, *108*, 936–942.
(c) Baker-Hawkes, M. J., Billig, E., & Gray, H. B. (1996). *J. Am. Chem. Soc.*, *88*, 4870–4875.

[16] (a) Abdallah, D. J., Sirchio, S. A., & Weiss, R. G. (2000). *Langmuir 16*, 7558–7561.
(b) Broadhurst, M. G. (1962). *J. Res. NBS. A. Phys. Chem.*, *66A*, 241–249.
(c) Teare, P. W. (1959). *Acta Cryst.*, *12*, 294–300.
(d) Shearer, H. M. M. & Vand, V. (1956). *Acta Cryst. 9*, 379–384.

[17] Barbera, J., Levelut, A. M., Marcos, M., Romero, P., & Serrano, J. L. (1991). *Liq. Cryst.*, *10*, 119–126.

[18] Sudhölter, E. J. R., Engberts, J. B. F. N., & de Jeu, W. H. (1982). *J. Phys. Chem.*, *86*, 1908–1913.

[19] (a) Tschinkl, M., Bachman, R. E., & Gabbaï, F. P. (1999). *J. Organomet. Chem.*, *582*, 40–44.
(b) Desiraju, G. R. (1997). *J. Chem. Soc., Chem. Commun.*, 1475–1482.

[20] (a) Connick, W. B., Marsh, R. E., Schaefer, W. P., & Gray, H. B. (1997). *Inorg. Chem.*, *36*, 913–922.
(b) Aullón, G., Alemany, P., & Alvarez, S. (1996). *Inorg. Chem.*, *35*, 5061–5067.

[21] Perrin, D. D. & Armarego, W. L. F. (1988). *Purification of Laboratory Chemicals;* 3rd ed. (New York: Pergamon Press).

[22] Pray, A. R. (1990). *Anhydrous Metal Chlorides*, Vol. 28, Angelici, R. J. (Ed.), (New York: John Wiley & Sons Inc.): pp. 321–323.

[23] Sasse, W. H. F. (1973). *Org. Synth. Coll.*, *5*, 103–107.
[24] Garelli, N. & Vierling, P. (1992). *J. Org. Chem.*, *57*, 3046–3051.
[25] Testaferri, L., Tiecco, M., Tingoli, M., Chianelli, D., & Montanucci, M. (1983). *Synthesis*, 751–755.
[26] (a) Thiemann, T. & Vill, V. (1998). *Handbook of Liquid Crystals*, Vol. 1, Demus, D., Goodby, J., Gray, G. W., Speiss, H.-W., & Vill, V. (Eds.), (Weinheim: Wiley-VCH) Chap. 4, p. 107.
[27] Broomhead, J. A. & Dwyer, F. P. (1961). *Aust. J. Chem.*, *14*, 250–252.
[28] Bachman, R. E. & Andretta, D. F. (1998). *Inorg. Chem.*, *37*, 5657–5663.
[29] (a) Blessing, R. H. (1995). *Acta Crystallogr., Sect. A*, *51*, 33–38.
(b) Sheldrick, G. M. (1996). SADABS, Universität Göttingen, Göttingen, Germany.
[30] (a) *SHELXTL-PC*, 5.10 ed.; (1998). (Madison, WI: Bruker-Analytical X-ray Services).
(b) Barbour, L. (1999). *XSEED*, online at http://www.xseed.com